

Reprinted with permission from: Postic I, Sheardown H. Altering the release of tobramycin by incorporating poly(ethylene glycol) into model silicone hydrogel contact lens materials
JOURNAL OF BIOMATERIALS SCIENCE, POLYMER EDITION 2019, VOL. 30, NO. 13,
1115–1141 <https://doi.org/10.1080/09205063.2019.1580663> ©

Altering the release of tobramycin by incorporating poly(ethylene glycol) into model silicone hydrogel contact lens materials

Ivana Postic and Heather Sheardown

Department of Chemical Engineering, McMaster University, Hamilton, Ontario, Canada

ABSTRACT

Delivery of drugs from contact lens materials is attractive for a number of reasons. However, the controlled delivery of hydrophilic drugs can be difficult to achieve due to the burst release of drug that is associated with materials of high water content, such as hydrogels. Silicone hydrogels have significant potential for drug delivery due to their increased hydrophobicity and the tortuous nature of the pores, overcoming some of the limitations associated with conventional hydrogel materials. The aim of this study was to examine the potential of model poly(ethylene glycol) (PEG) containing silicone hydrogels for delivery of hydrophilic aminoglycoside antibiotics. It was hypothesized that PEG, a polymer that has seen extensive use in biomedical applications, will provide in addition to hydrophilicity and protein repulsion, a mechanism for controlling the delivery of this hydrophilic antibiotic. PEG was combined with the macromer TRIS to create the model silicone hydrogel materials. The optical and physical properties of the novel TRIS-co-PEG silicone hydrogels exhibited excellent transparency, appropriate refractive index and high transmittance indicating minimal phase separation. Desirable properties such as wettability and protein repulsion were maintained across a wide range of formulations. The water content was found to be highly correlated with the ethylene oxide content. Drug release could be influenced through PEG content and was found to fit Higuchi-like kinetics. Overall, the study demonstrates that incorporation of PEG into a model silicone hydrogel could be used to control the release of a hydrophilic compound. Data suggests this is related to the unique structure and properties of PEG, which alter the types of water found in each formulation and the water content.

KEYWORDS

Drug delivery; silicone hydrogels; contact lens; poly(ethylene glycol)

CONTACT Heather Sheardown, sheadow@mcmaster.ca, McMaster University, 1280 Main Street West, Hamilton, Ontario, L8S4L8, Canada

Introduction

In order to provide better therapeutic efficacy and safety, drug delivery systems have been widely applied in pharmaceutical formulations. Hydrogels in particular have received a great deal of attention as potential candidate materials for controlling the release of drugs [1, 2]. These water swollen hydrophilic network polymers impart their controlled release by acting as a partition through which the drug compound of interest must diffuse [3]. True controlled release of hydrophilic compounds, however, can be very difficult to attain. This is primarily due to burst release associated with a hydrophilic drug that occurs almost immediately upon placing the drug-loaded device in contact with an aqueous solution [3–6]. In addition, protein deposition can lead to fouling, which can alter drug release rates and result in inflammation [7].

Despite these limitations, hydrogels remain one of the most widely used type of biomaterials due to their biocompatibility [8], versatility [9], and low material cost [10, 11]. While hydrogels remain the standard for drug delivery in numerous clinical applications [12, 13], substantial research has been devoted to the development of strategies to overcome the limitations of these materials. For example, increasing the crosslinking density within a hydrogel can reduce the rate of hydrophilic drug release [9, 14]. Covalent tethering of a drug via hydrolysable or biodegradable linkers is another strategy for controlling the release of the drug [15, 16]. These approaches may not, however, be optimal for clinical translation due to the changes in the desired physical properties of the material (e.g. transparency, contact angle) that may be the result of these modifications [17, 18].

An alternate strategy is to use physical interactions between the polymer and the drug to tune drug release. This has been frequently seen in molecular imprinting, where physical interactions (such as ionic and hydrogen-bonds) between the polymer and drug are used to first assemble the polymer in a way that creates ‘pockets’ of drug. These ‘pockets’/drug templates can then increase drug uptake and slow release of the polymer [19–23]. These interactions are often ionic and require the incorporation of ionisable polymers. However, increased surface charge on a material can lead to increased protein deposition and other deleterious effects [24, 25]. Protein deposition can subsequently lead to undesirable activation of inflammatory processes and ultimately in the

rejection of the material by the body [26, 27]. Although ionic polymers tend to be non-toxic and excellent for oral drug delivery, their widespread application as hydrogel biomaterials may not be optimal, especially where protein deposition may increase the risk of complications such as in blood contacting devices and contact lenses.

Outside of molecular imprinting, a physical interaction that has not been widely explored for drug delivery alone is hydrogen-bonding between the polymer and drug, likely due to this bond being weaker than ionic bonds. There are only a few examples where this bonding has been used alone for drug delivery. For instance, Papageorgiou et al. were able to demonstrate hydrogen bonding between solid dispersions of hydrophilic drug and chitosan matrices [28]. This physical interaction led to a slowed drug release and hydrogel formulations with minimal burst release [28]. The release data suggest that the very small amount of drug available at the surface releases more easily than the deeply embedded drug, leading to a smaller burst release [28]. Ozeki et al. were similarly able to show that hydrogen bonding between solid dispersions of a drug in poly(ethylene glycol)-containing matrices altered drug release rates [29]. Despite these studies indicating that hydrogen bonding can control drug release, a limitation of these formulations is the loading of drugs as solid dispersions within the matrices which may lead to changes in the physical properties of the hydrogels as the drug is released (such as changes in crystallinity leading to changes in elasticity or mechanical strength) [30–33].

In this work, it was hypothesized that by incorporating the hydrogen bonding potential of poly(ethylene glycol) (PEG) as the hydrophilic component of silicone hydrogel materials, burst release of hydrophilic drugs loaded by soaking can be reduced, and more gradual release can be attained. Specifically, similar to PEG binding with water, which can have three states (tightly bound, loosely bound and free [34]), it was hypothesized that hydrogen binding between PEG and a hydrophilic drug will occur and that this will lead to more gradual release of the drug. A silicone hydrogel system was chosen for this study, as they are currently the most commonly prescribed contact lens materials [35], and they have numerous properties that make them excellent biomaterials including high oxygen permeability and, with appropriate surface modification, minimal protein deposition. Further, the siloxane component of these materials could provide a physical barrier to drug transport, slowing drug release compared to more conventional hydrogel materials. In this work, it is

hypothesized that by incorporating the hydrogen bonding potential of poly(ethylene glycol) (PEG) as the hydrophilic component of silicone hydrogel materials, control over drug release can be achieved, particularly for hydrophilic drugs. While there is interest in using these materials for drug release, they have, somewhat surprisingly, not been widely successful in their commercialization for this purpose.

In addition to potential drug influencing properties, PEG is of particular interest in this application as it has the unique property of being able to hydrogen bond 2-3 water molecules for every ethylene oxide unit [36, 37]. Its high chain flexibility adds to the ability of PEG to create a large cage of hydrogen-bonded water around it [36, 37]. Steric hindrance then produces the protein repelling properties that are desirable in biomedical applications [38]. Notably, PEG is known to maintain many of its freechain characteristics when incorporated into a hydrogel. In these applications, the strong hydrogen-bonding ability of PEG is able to mask hydrophobic surfaces that can be prone to protein adsorption [39, 40], allowing for the creation of surfaces with high surface energy and low protein adsorption.

Thus, in order to test the hypothesis that PEG containing silicone hydrogels could be used to control drug release via hydrogen-bonding, the release of highly hydrophilic drugs (tobramycin and amikacin) was tested using model silicone hydrogels composed of TRIS-co-PEG. Tobramycin is specifically used in ocular applications as an antibiotic eye drop [41], but due to the fast washout times, it must be applied multiple times each day for efficacy and therefore would benefit from controlled release to maximize patient compliance [42] and improve drug bioavailability [43]. In addition to drug release, polymer properties including surface and bulk characteristics were examined.

Materials

(3-methacryloyloxypropyl)tris(trimethylsiloxy) silane (TRIS), poly(ethylene glycol) methyl ether methacrylate (PEG, with M_n of 500 or 300), ethylene glycol dimethacrylate (EDGMA), isopropyl alcohol, inhibitor remover beads, tobramycin ($\geq 98\%$), fluorescamine ($\geq 98\%$), amikacin (European pharmacopeia standard), lysozyme from chicken egg white, bovine serum albumin, and sodium dodecyl sulfate were purchased from Sigma-Aldrich (Oakville, ON). The photoinitiator 1-hydroxy-cyclohexyl-phenylketone (Irgacure[®] 184) was generously donated by BASF Chemical Company

(Vandalia, IL). 10x phosphate-buffered saline was obtained from Bioshop Canada Inc. (Burlington ON) and diluted to 1x for experiments. The UV-permeable acrylic mold (Plexiglass^{VR} G-UVT) was generously donated by Altuglass International (Bristol, PA). A Cure Zone 2 CON-TROL-CURE (Chicago, IL) chamber with a 400 W UV lamp and 365 nm wavelength light was used for polymer preparation. A Tecan Infinite^{VR} M1000 PRO plate reader spectrophotometer was used for all spectrophotometry. A Hyperion 3000 microscope (Bruker Corporation Billerica, MA) was used for FTIR measurements. SEM was performed using a FEI-Magellan 400, XHR FE-SEM. Surface wettability of each material was determined using contact angle measurements made on a Dataphysics OCA20 goniometer (Dataphysics Instruments GmbH Filderstadt, Germany). An Atago Pal-1 pocket refractometer (Atago Co LTD., Japan) was used to measure the refractive index of the materials. Proton NMR was performed on a Bruker AV 600 spectrometer at 600MHz. CryoTEM was performed on a JOEL 1200EX TEMCAN. Mechanical testing was performed on an Instron 4411 Universal Tester.

Methods

Silicone hydrogel synthesis

Macromers and crosslinkers were passed through a syringe column containing inhibitor remover prior to polymerization. The compositions of the polymers prepared are summarized in [Tables 1](#) and [2](#). Note that the molar ratios presented in [Table 1](#) are based on the full chain length of the PEG rather than the repeat unit of ethylene oxide.

Table 1. Composition of silicone hydrogel formulations (mol%).

Formulation	Ratio	Macromer			Crosslinker EGDMA	Inclusion in study
		TRIS	PEG ₅₀₀	PEG ₃₀₀		
TRIS-co-PEG ₅₀₀	1 : 1	48.5	48.5	–	3	+
TRIS-co-PEG ₃₀₀	1 : 1	48.5	–	48.5	3	+
TRIS-co-PEG ₅₀₀	7 : 3	67.9	29.1	–	3	+
TRIS-co-PEG ₃₀₀	7 : 3	67.9	–	29.1	3	+
TRIS-co-PEG ₅₀₀	3 : 7	29.1	67.9	–	3	–
TRIS-co-PEG ₃₀₀	3 : 7	29.1	–	67.9	3	–

Table 2. Composition of silicone hydrogel formulations (wt%).

Formulation	Ratio	Macromer		
		TRIS	PEG ₅₀₀	PEG ₃₀₀
Tris-co-PEG ₅₀₀	0.85 : 1	45.8	54.2	
Tris-co-PEG ₃₀₀	1.41 : 1	58.5		41.5
Tris-co-PEG ₅₀₀	1.98 : 1	66.4	33.6	
Tris-co-PEG ₃₀₀	3.29 : 1	76.7		23.3

The crosslinker was not included in these calculations for simpler ratio visualization.

200mL (2.61mol) of isopropyl alcohol was added to the macromer solution to facilitate mixing between PEG and TRIS as it was found that macromer solutions prepared without IPA had visible phase separation, and incomplete polymerization. In addition, the length of PEG macromers were selected to be as small as possible as it was hypothesized that increased phase separation would result from the use of longer chain PEGs. Following mixing, 7.35mg of photoinitiator (Irgacure^{VR} 184) was added. The resulting solution was thoroughly mixed by vortexing and subsequently transferred using a 20 gauge needle to a custom hydrogel-mold (polystyrene sheets separated by a Teflon spacer). The mold was then placed in the UV chamber and activated with light at 365 nm for a period of 15 minutes.

The cross-linked hydrogel materials were then soaked in 20mL of IPA for 4 x 30min then in 20mL water for 2 x 30minutes to remove residual unreacted components and IPA. Hydrogels were placed in fresh distilled water for long-term storage. As noted in Table 2, crosslinked formulations containing TRIS-co-PEG (3:7) were not included in this study, as they were determined to be too fragile to be handled. Figure 1 shows the reaction process.

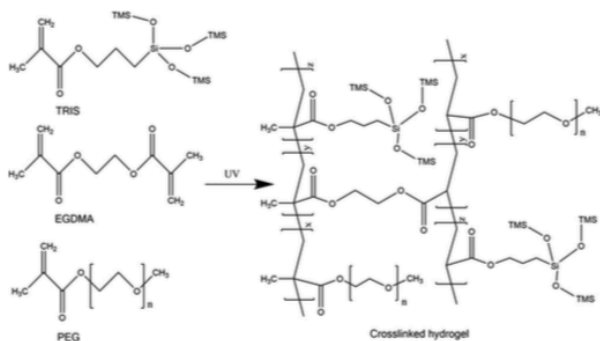


Figure 1. Schematic depicting the reaction between macromers and crosslinker to form the novel hydrogel materials. n: repeating ethylene oxide units corresponding to 300 or 500 molecular weight PEGs. x,y,z: varying macromer ratios that exist within the hydrogels. TMS: trimethylsilyloxy.

ATR-FTIR

Attenuated-total reflection Fourier transform infrared spectroscopy (ATR-FTIR) was used to evaluate the UV polymerization procedure by characterizing the materials for the presence of specific chemical groups present in the TRIS and PEG macromers.

NMR

Extracted hydrogels were dried overnight at 37 °C. Macromers (with inhibitors removed) and dried hydrogels were solvated in CDCl₃ and ¹H NMR was performed at room temperature.

SEM

Scanning-electron microscopy (SEM) of the materials was performed to examine the surface composition of the hydrogels and surface roughness. All materials were examined on glass-polished steel supports to avoid the formation of dehydration artifacts. Two states of materials were compared: (1) Dry materials formed immediately after polymerization, and (2) hydrated materials dehydrated on the glass-polished supports. Dehydration was performed at 37 °C.

Contact angle

Surface wettability of the hydrogels was measured using the captive bubble method to ensure hydrogels remained hydrated during measurement, and that artifacts from material dehydration were avoided. Captive bubble measurements have also been determined to be more clinically relevant than sessile drop measurements [44]. However, given that sessile drop angles are more commonly reported and understood, the captive bubble contact angles are reported similarly to sessile drop angles (180-h) for easier comprehension of the material hydrophilicity.

Protein adsorption

Protein deposition studies were performed to assess the non-fouling effect of PEG incorporation in these model contact lens materials. Lysozyme and albumin were chosen as model proteins for study. Lysozyme is the most abundant protein in the tear film; albumin has been touted as having a passivation effect and is also abundant in the tear film, particularly during times

of stress such as would be the case in an inflamed or infected eye.

Four samples of each material (1/4") were placed in 0.2mL of 1mg/ml protein solution (lysozyme or albumin) radiolabeled with 10% Iodine¹²⁵. Samples were incubated in protein solution for 3hours at room temperature. The hydrogels were then rinsed three times for five minutes each in 0.2mL of PBS in order to remove any loosely bound protein. Samples were then carefully dabbed with a KimWipe to remove excess surface droplets. Adsorbed protein on the samples was measured by reading samples for 5minutes using a gamma counter (1470 Wallac Wizard; PerkinElmer, Woodbridge, ON).

Mechanical testing

The strength and elasticity of the materials was measured on materials formed into a barbell mold (9 mm width, 35 mm grip distance). A 50 N load cell was used to collect measurements and speed was 10 mm/min.

Light transmittance

Materials were tested for transparency by measuring the light transmittance over the UV and visible spectrum (200–400, 400–700nm, respectively). PBS-hydrated discs were placed on the bottom of a 96-well plate with an overlay of 100mL of PBS and measured using a spectrophotometer.

Refractive index

The refractive index of the materials swollen in 300 mL of PBS was measured at ambient temperature using a pocket refractometer.

TEM

Transmission electron microscopy was performed on materials hydrated in water then cut with a microtome while under cryogenic conditions. TEM was performed in order to better visualize the potential phase separation between TRIS and PEG within each material.

Water content

Samples a quarter-inch in diameter were swollen in distilled water for a minimum of 24hours at room temperature, subsequently removed and excess water gently removed using a KimWipe. The sample was then weighed and

placed in a 37-C oven until completely dry. The dry samples were then weighed and the equilibrium water content was calculated using Equation 1.

$$EWC (\%) = \frac{\text{mass of hydrated gel (mh)} - \text{mass of dry gel (md)}}{\text{mass of hydrated gel (mh)}} \cdot 100\% \quad (1)$$

Differential scanning calorimetry

Hydrogels swollen in distilled water were placed into aluminum pans. Lids were placed immediately and the pans were sealed to prevent evaporation. DSC was performed using a DSC200 (TA Instruments, Newcastle, DE) by ramping temperature from -40 -C to 15 -C at 5 -C/min. The free/bulk/freezable water, loosely bound/intermediate water and tightly bound/non-freezable water were calculated according to Ping et al. [45]. Water was chosen as the solvent rather than PBS as it is the standardized method for characterizing hydrogels in the literature, but also to achieve a more direct understanding of any relationship between PEG and water molecules, and for relating resulting data to the equilibrium water content of each hydrogel. DSC thermograms were normalized to the mass of water in each gel (product of EWC and mass of hydrated material).

Drug loading and release

Phosphate-buffered saline, pH 7.4, was sterile-filtered prior to use by passing it through a 0.2 IM filter. Four 1/4" samples of each material were equilibrated in PBS for at least 24hours. The samples were then loaded with drug solution by placing them in 1mL of 5mg/mL tobramycin or amikacin (solvated in PBS) for 24hours. Samples were then carefully wiped using a KimWipe to ensure all surface drops were removed. Drug release was performed by placing samples individually in 0.5mL of PBS in a VWR shaking incubator (37-C, 100rpm). PBS was replaced at predetermined timepoints over 6 hours and at 24 hours.

Drug quantification

For quantification of the released drug, an adapted literature procedure involving conjugation of fluorescamine through the free amine and subsequent fluorimetry was performed [46–48]. Within each well, 150mL of release solution from the study was incubated with 50mL of 5mg/mL fluorescamine dissolved in DMSO. The fluorescent compound was measured at

excitation/emission wavelengths set to 380/480nm. The assay was performed in black 96-well plates in order to reduce background fluorescence and prevent cross-talk between wells.

Statistical analysis

A one-factor analysis of variance was used to analyze the equilibrium water content and contact angle. A Tukey test was performed post-hoc when significant differences were identified ($p < 0.05$). All error bars represent standard deviation.

Results

Confirmation of synthesis

ATR-FTIR

In order to confirm the conjugation of TRIS and PEG, ATR-FTIR was performed on each of the samples. The FTIR spectra are displayed in [Figure 2](#).

There were 6 regions of peaks identified in the spectra (labelled A-F). C and D are peaks that correspond to the bonds of Si-O-R and Si-CH₃, respectively. The ether bonds of PEG are also found within this region (1000–1300) and are not distinguishable as they likely directly overlap with silicone peaks. Regions A and F indicate the presence of PEG. Region F corresponds to the O-H bond of water. Region A (the “fingerprint region”) shows the presence of PEG, as this region is altered in the presence of PEGs with different molecular weights. Specifically, PEG₅₀₀ has a unique fingerprint in comparison to PEG₃₀₀. Peaks in the B region correspond to the benzene groups of residual photoinitiator.

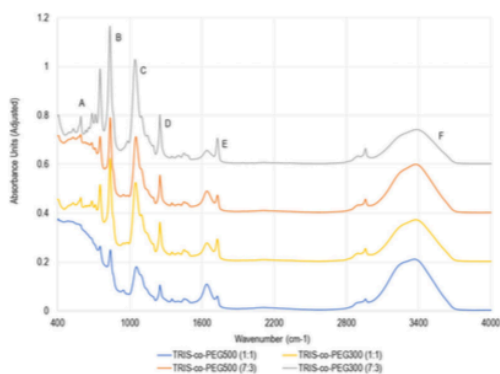


Figure 2. FTIR spectra of TRIS-co-PEG materials. *Note, baseline for black is 0 A.U, black-dash is 0.2 A.U, grey is 0.4 A.U, grey-dash is 0.6 A.U.

NMR

The ^1H NMR results of the macromers and hydrogels are reported in [Table 3](#). Full spectra are available in [Supplementary Information](#). Macromer spectra were as expected, and crosslinked hydrogels showed some peak broadening as was expected.

Due to the varying molecular weights of PEG and macromer molar ratios, the expected number of protons (based on the macromere NMR peak integration performed in spectra from [Table 3](#)), was compared with the measured number of protons (based on the hydrogel NMR spectra, and using the PEG peak as the reference value). These results seen in [Table 4](#) confirm that the hydrogels were successfully polymerized at the input molar ratios. Some difference between expected and measured proton numbers was expected and is seen (due to the broadened peaks in the crosslinked, polymerized hydrogels).

Table 3. ^1H NMR shifts of macromers and hydrogels in CDCl_3 . Hydrogel shifts are reported only for the EO chain and TMS for ease of reading.

Macromer	^1H NMR (CDCl_3 , 600 MHz) δ	Hydrogel	^1H NMR (CDCl_3 , 600 MHz) δ (for EO chain, TMS)
TRIS	7.16 (s, solvent peak); 6.00 (q, 1H, $\text{CH}_2=\text{C}$); 5.44 (t, 1H, $\text{CH}_2=\text{C}$); 3.98-4.01 (m, 2H, OCH_2); 1.85 (t, 3H, CH_3); 1.59 (q, 2H, CH_2); 0.4 (m, 2H, CH_2Si); 0 (s, 27H, TMS)	TRIS-co-PEG ₅₀₀ (1:1)	2.4-4.41 (m, 33H, $(\text{CH}_2\text{CH}_2\text{O})_n$); 0.53-0.86 (s, 27H, TMS)
PEG ₅₀₀	7.29 (s, solvent peak); 6.10 (s, 1H, $\text{CH}_2=\text{C}$); 5.55 (d, 1H, $\text{CH}_2=\text{C}$); 4.26-4.29 (m, 2H, OCH_2); 3.51-3.75 (m, 33H, $(\text{CH}_2\text{CH}_2\text{O})_n$); 3.35 (s, 3H, PEG- CH_3); 1.92 (s, 3H, CH_3)	TRIS-co-PEG ₃₀₀ (1:1)	2.31-4.88 (m, 18H, $(\text{CH}_2\text{CH}_2\text{O})_n$); 0.52-0.59 (s, 28H, TMS)
PEG ₃₀₀	7.29 (s, solvent peak); 6.12 (s, 1H, $\text{CH}_2=\text{C}$); 5.57 (d, 1H, $\text{CH}_2=\text{C}$); 4.27-4.31 (m, 2H, OCH_2); 3.52-3.80 (m, 16.16H, $(\text{CH}_2\text{CH}_2\text{O})_n$); 3.37 (s, 3H, PEG- CH_3); 1.94 (s, 3H, CH_3)	TRIS-co-PEG ₅₀₀ (7:3)	2.51-4.59 (m, 33H, $(\text{CH}_2\text{CH}_2\text{O})_n$); -0.71-0.49 (s, 59H, TMS)
EGDMA	7.29 (s, solvent peak); 6.12 (s, 1H, $\text{CH}_2=\text{C}$); 5.57 (d, 1H, $\text{CH}_2=\text{C}$); 4.27-4.31 (m, 2H, OCH_2); 3.52-3.80 (m, 16.16H, $(\text{CH}_2\text{CH}_2\text{O})_n$); 3.37 (s, 3H, PEG- CH_3); 1.94 (s, 3H, CH_3)	TRIS-co-PEG ₃₀₀ (7:3)	2.76-4.6 (m, 16H, $(\text{CH}_2\text{CH}_2\text{O})_n$); -0.93-0.60 (s, 66H, TMS)

Table 4. The structure of each hydrogel formulation is confirmed using ^1H NMR data.

	Expected # of Protons		Measured # of Protons	
	$(\text{CH}_2\text{CH}_2)_n$	TMS	$(\text{CH}_2\text{CH}_2)_n$	TMS
TRIS-co-PEG ₅₀₀ (1:1)	33	27	33	27
TRIS-co-PEG ₃₀₀ (1:1)	16	27	16	25
TRIS-co-PEG ₅₀₀ (7:3)	33	63	33	59
TRIS-co-PEG ₃₀₀ (7:3)	16	63	16	66

Surface properties

Surface morphology

The surface morphology of silicone hydrogels can demonstrate the presence of phase separation and provide an indication of surface roughness. Both factors are important in producing materials that are more biologically compatible, as exposure of the hydrophobic TRIS component on the surface can lead to protein denaturation, irritation, and inflammation.

The surface morphology was measured using SEM under two conditions: materials were either dry (tested after polymerization) or dehydrated (swelled in water then dehydrated) on the SEM stand. These conditions were tested in order to observe for the possibility of dehydration artifacts. Dehydrated samples are likely more accurate representations of the material surface in biological settings, as the presence of water is very likely to alter the position of macromer chains.

In [Figure 3](#), SEM images at 25,000X magnification are shown. The representative images were chosen because they captured defects in the material, indicating that the surfaces are in focus. With the exception of TRIS-co-PEG₅₀₀ (1:1), the materials were highly consistent and very smooth. TRIS-co-PEG₅₀₀ (1:1) was seen to have more channel like formations under dry conditions, with some faint waves after dehydration. There is no indication of artifacts from the dehydration process for hydrated materials.

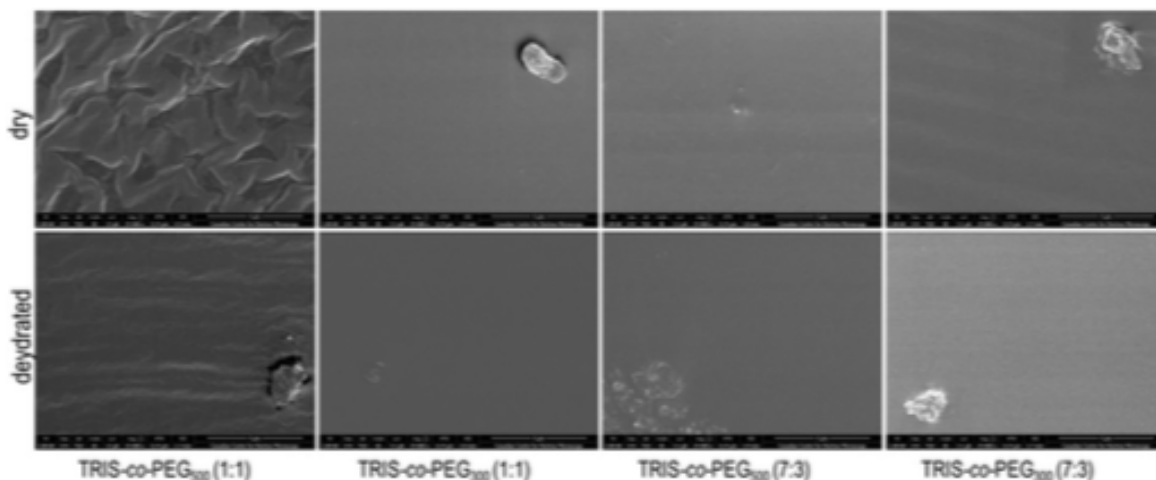


Figure 3. Surface morphologies of TRIS-co-PEG materials as observed using SEM. Representative images shown are taken at 25,000 \times magnification. The top row are materials which were imaged directly after polymerization and have not previously been hydrated. The bottom row are materials which have been soaked in water, then dehydrated on the SEM stand.

Contact angle

The surface hydrophilicity of a material can provide significant information on its potential applications. Highly hydrophobic materials may not be suitable for biomaterial applications, due to the potential for protein deposition and denaturation. The surface hydrophilicity was assessed using contact angle measurements and a protein deposition assay.

All materials were very hydrophilic at the surface (Table 5). The differences in contact angle across the materials was not significant ($p > 0.05$). This indicates that PEG is able to produce similar interactions with water on the material surface, regardless of the PEG concentration or molecular weight tested.

Surprisingly, TRIS-only materials showed to be hydrophilic as well. It is known that TRIS macromers are hydrophobic, however, when polymerized it is possible that the conformation of the side chains impacts the surface hydrophilicity. Specifically, the contact angles may show a hydrophilic surface due to the hydrophobic trimethylsiloxane chain ends being entropically more favoured to be tucked inside of the material. At the same time, the carbonyl of the polymerized methacrylate backbone is preferentially exposed to the surface, where the oxygen can hydrogen-bond with two water molecules and form the hydrophilic surface that was observed.

Table 5. Contact angles of TRIS-co-PEG materials (n = 3).

Material (mol ratio)	Contact Angle (°)
TRIS-co-PEG ₅₀₀ (1:1)	35.02 ± 4.86
TRIS-co-PEG ₃₀₀ (1:1)	40.66 ± 5.19
TRIS-co-PEG ₅₀₀ (7:3)	46.11 ± 6.08
TRIS-co-PEG ₃₀₀ (7:3)	40.46 ± 0.87
TRIS-only	55.09 ± 9.75

Protein adsorption

Protein adsorption measurements further confirm the hydrophilicity of the material surface. After incubation in 1 mg/mL of protein (hen egg lysozyme or bovine serum albumin), there was less than 1 mg protein/cm² adsorbed (Figure 4).

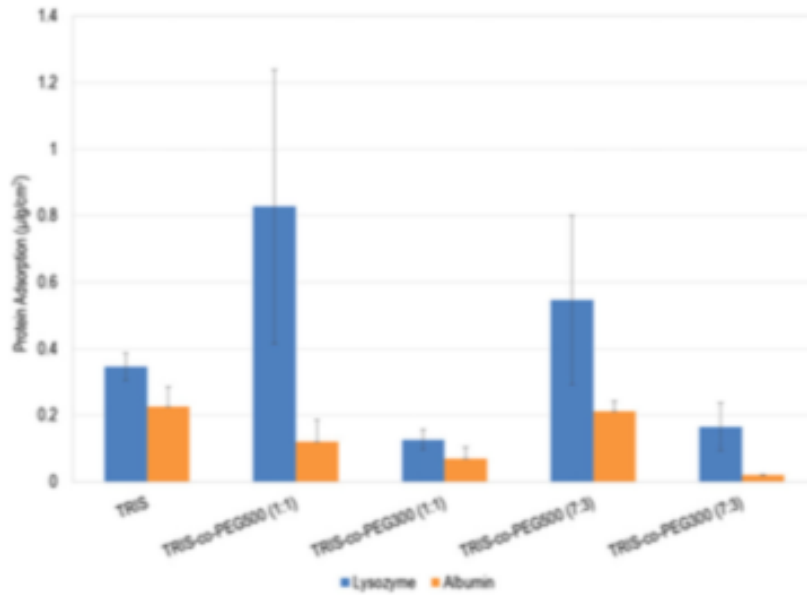


Figure 4. Adsorbance of lysozyme or bovine serum albumin onto the hydrogels (stdev, n = 4).

Notably, lysozyme (14.3kDA) is the smaller of the two proteins and seen to be more greatly sorbed within the materials, likely because it can diffuse into the material and become sorbed there, instead of being adsorbed only on the surface. The highest lysozyme sorption is seen with the materials with highest EWC (see [Table 7](#)). TRIS-only material was included for comparison, and results show that the materials with PEG₃₀₀ (lowest EWC) show lower protein adsorption than TRIS-only material, indicating the protein repelling property of PEG. The data also suggests that TRIS-only materials swell/retain water (due to the increased lysozyme sorption) and this data was confirmed in EWC/swelling studies shown later ([Table 7](#)).

Albumin-adsorbed materials show fairly consistent and low protein adsorption (<0.1mg/cm²). The lower adsorption (in comparison to lysozyme) is attributed to the lower molecular packing due to the larger size of albumin, and lowered ability to diffuse into the material.

Overall, this data indicates that TRIS-co-PEG materials show good surface wettability, based on its low overall protein sorption and surface contact angle.

Table 6. Refractive indexes of TRIS-co-PEG materials.

	Refractive Index
TRIS-co-PEG ₅₀₀ (1:1)	1.3326 ± 0.0002
TRIS-co-PEG ₃₀₀ (1:1)	1.3329 ± 0.0001
TRIS-co-PEG ₅₀₀ (7:3)	1.3328 ± 0.0001
TRIS-co-PEG ₃₀₀ (7:3)	1.3329 ± 0.0001

Table 7. The EWC and swelling of each formulation was statistically ($p < 0.05$) significantly different from the other ($n = 4$).

	Equilibrium Water Content (%)	Swelling Ratio (%)
TRIS-co-PEG ₅₀₀ (1:1)	57.88 ± 1.37	137.6 ± 7.69
TRIS-co-PEG ₃₀₀ (1:1)	18.75 ± 2.09	23.14 ± 3.12
TRIS-co-PEG ₅₀₀ (7:3)	28.62 ± 2.94	40.27 ± 5.88
TRIS-co-PEG ₃₀₀ (7:3)	5.72 ± 1.52	6.09 ± 1.71
TRIS-only	6.30 ± 1.17	6.74 ± 1.34

Bulk properties

In order to fully characterize the influence of PEG structure on the hydrogel, the bulk properties of the material were assessed through measurements of tensile properties, optical qualities and water content.

Tensile testing

The tensile strength and elasticity of a biomaterial is important for both the handling of the material and its successful application at the site of use. For example, for contact lenses, the materials must be strong enough to be handled without damage by a patient, and not too soft that they bend when blinking forces are applied [49, 50]. Figure 5 shows the strength and elastic modulus of the TRIS-co-PEG materials. The PEG₅₀₀ (7:3) formulation shows both the greatest modulus and strength. The PEG₃₀₀ (7:3) formulation shows the lowest modulus. PEG₃₀₀ (7:3) and PEG₅₀₀ (1:1) show the lowest strengths. This data is somewhat surprising given the knowledge that siloxanes provide strength due to the Si-O bonds, thus this unique data is later further explored in the context of the hydrated material and its relationship with water. Still, the modulus data is within range of reported values for conventional hydrogels in the literature [51, 52].

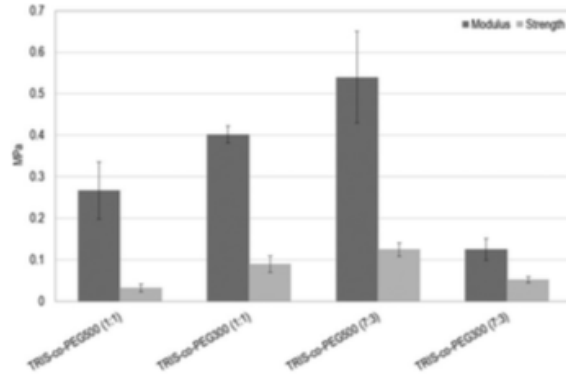


Figure 5. Mechanical properties of materials (stdev, n = 4).

Optical qualities

Material transparency is important to evaluate because it can provide information on the polymerization efficiency and optical qualities which may be important in certain biomedical applications such as ophthalmology. It was hypothesized that the materials may be translucent or opaque, due to possibility for phase separation between the hydrophobic TRIS and hydrophilic PEG. However, all the materials were highly transparent when hydrated in PBS as seen in Figure 6. PEG₃₀₀ (7:3) materials showed opacity when hydrated only in water, indicating that the PBS salts help to create more favorable PEG conformations for less phase separation between the short-chain PEG and the high TRIS content.

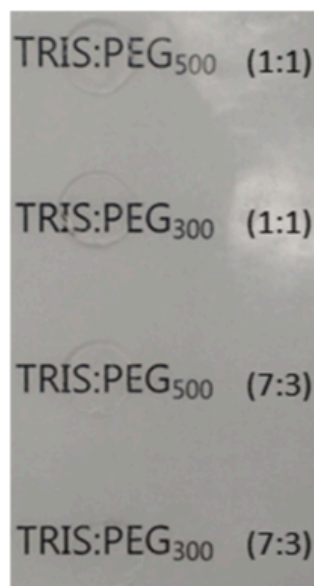


Figure 6. Photograph image of novel TRIS-co-PEG hydrogels swollen in PBS.

The optical qualities were further confirmed by measuring the refractive index of the materials. The refractive indexes of the materials were all within 0.02% of the refractive index of PBS alone, and within measurement error of the device (± 0.00005), as described in [Table 6](#). This data is lower than that of commercial corrective lenses [53], however it does not impeded further study of the materials as model silicone hydrogels for understanding the structure-function properties of PEG.

The light transmittance of the materials ([Figure 7](#)) was measured across UV and visible wavelengths. All materials transmitted about 100% of light across the visible spectrum. TRIS-co-PEG₅₀₀ (7:3) materials showed slightly lower (~95%) transmittance across the visible spectrum in comparison to the other materials. All materials similarly transmitted UV light across the 200-400nm wavelengths, with a sharp rise in transmittance with increasing wavelength.

Overall, despite the opposing solubilities of the macromers, all materials were highly transparent in terms of visual clarity, refractive index and transmittance across the visible spectrum when hydrated in PBS.

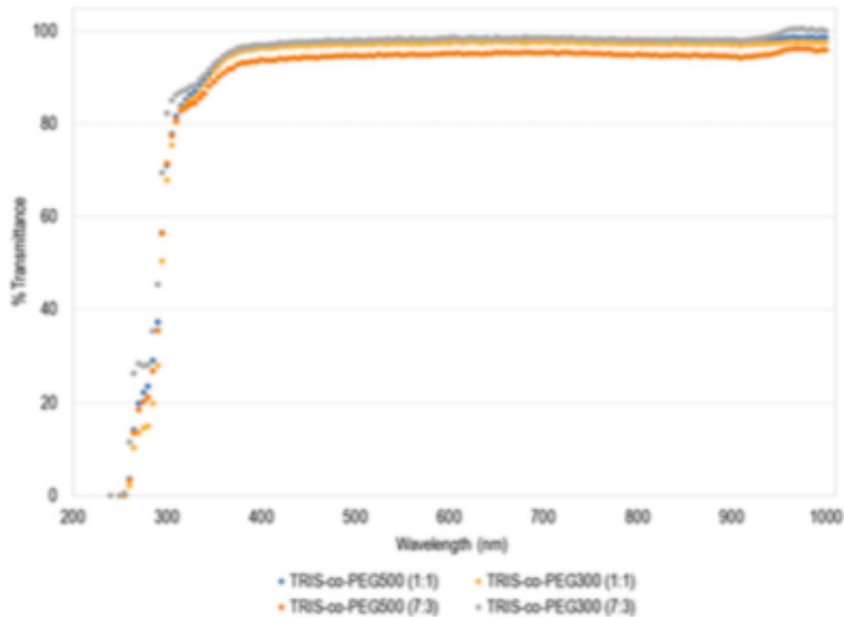


Figure 7. The light transmittance of each material across the UV and visible spectrums ($n = 3$).

TEM

The internal structure of the hydrogels is seen through TEM imaging in [Figure 8](#). Even at high magnification (30,000x), large phase separation is not seen, rather, there is some visible nanometer-sized phase separation. The size of this phase separation is not dissimilar from that seen in TRIS-only materials containing EGDMA crosslinker. Overall, this data provides support for the optical material properties, as the minimal phase separation that is seen does not impede the transport of light through the material.

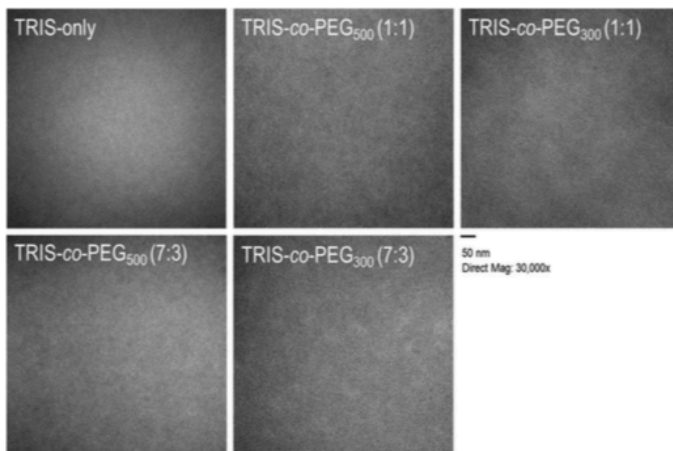


Figure 8. cryoTEM images of materials at 30,000x magnification.

Equilibrium water content and swelling

The potential to hold large amounts of water make hydrogels attractive in a variety of medical applications, allowing for permeation of nutrients and other small molecules. In [Table 7](#), the equilibrium water content and swelling can be seen to vary significantly across the material formulations.

As expected, the highest water content/swelling was seen with the longest PEG chain (PEG₅₀₀) at the highest concentration (1:1 TRIS) while the lowest water content/swelling was seen with the shortest PEG chain (PEG₃₀₀) at the lowest PEG concentration (3:7 TRIS). Other formulations had intermediate water contents/swelling.

Relationship with water

The relationship between EWC/swelling and PEG

Given the understanding that PEG is responsible for the hydrophilicity of the material, and that each ethylene oxide subunit of PEG can hydrogen-bond 2-3 water molecules, the relationship between EWC/swelling and the number of EO moles per material was investigated ([Figure 9](#)). The number of EO moles per material is the product of the moles of PEG per material and the average number of EO units per PEG chain (9 for PEG₅₀₀ and 4.5 for PEG₃₀₀). There is a high, linear correlation ($R^2 \approx 0.99$) with the EWC and a similarly linear correlation ($R^2 \approx 0.95$) with swelling.

This data supports the molecular relationship of PEG with water, and indicates an ability to control the EWC and swelling by altering the number of EO moles per material.

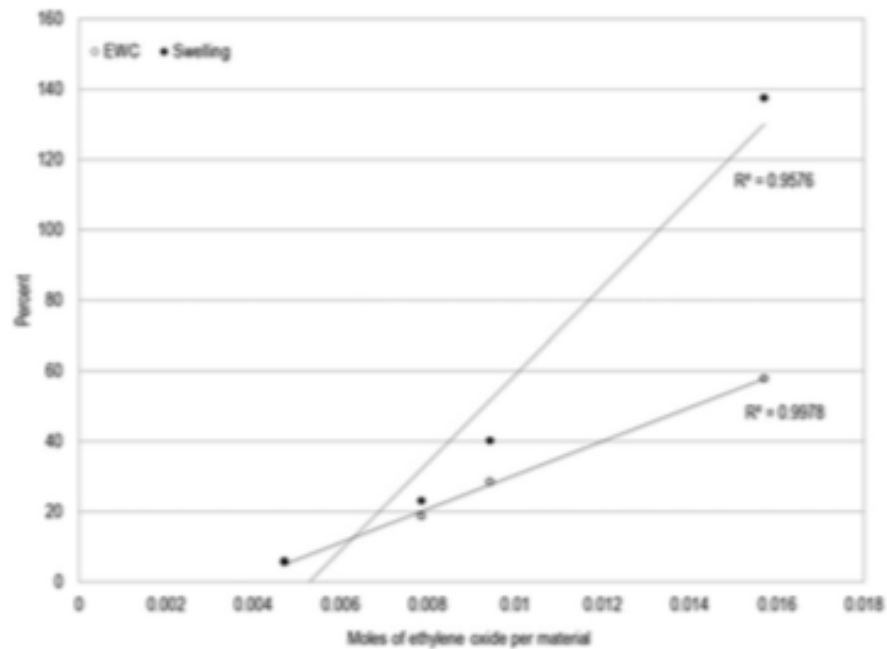


Figure 9. Equilibrium water content and swelling ratio of each formulation (n = 4).

DSC analysis of the types of water in each material

The type of water in each hydrogel can further provide information on the influence of PEG on material properties and the potential of the hydrogels for biomedical applications. Differential scanning calorimetry was performed on each of the formulations to determine the amount of free, intermediate/loosely-bound and non-freezable/ bound water in each hydrogel.

The DSC data (Figure 10) shows unique spectra for each hydrogel. Notably, intermediate water (melting at temperature lower than 0-C), is seen to some degree across all materials. Because this area of the curve for intermediate water is not distinct from that of the free water peak at 0-C, it is not possible to integrate it separately. However, visually, it can be observed that the amount of loose water is greatest in the PEG₅₀₀ (1:1) material, and lowest in the PEG₃₀₀ (7:3) material. Because the two peaks are not distinguishable, these integrated DSC peaks will thus be referred to as the ‘freezable’ water peak.

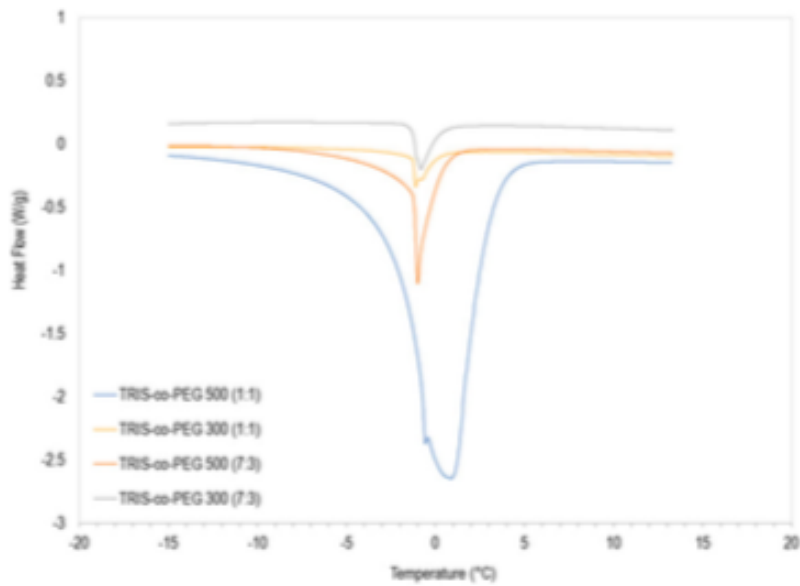


Figure 10. Representative DSC thermograms of materials (based on polymer and water weight).

Relationship between the types of water and PEG

The freezable and bound water were calculated according to Ping et al. [45] and placed in relationship to the amount of water in each hydrogel (EWC) as seen in Figure 11. The data show that the higher the EWC, the larger the amount of tightly bound water. In terms of the relationship to PEG molecular weight, formulations containing PEG₃₀₀ also showed the lowest amount of free water and formulations containing PEG₅₀₀ showed the greatest amount of tightly bound water. Therefore together the DSC and EWC data demonstrate an influence of the structure of PEG on material properties.

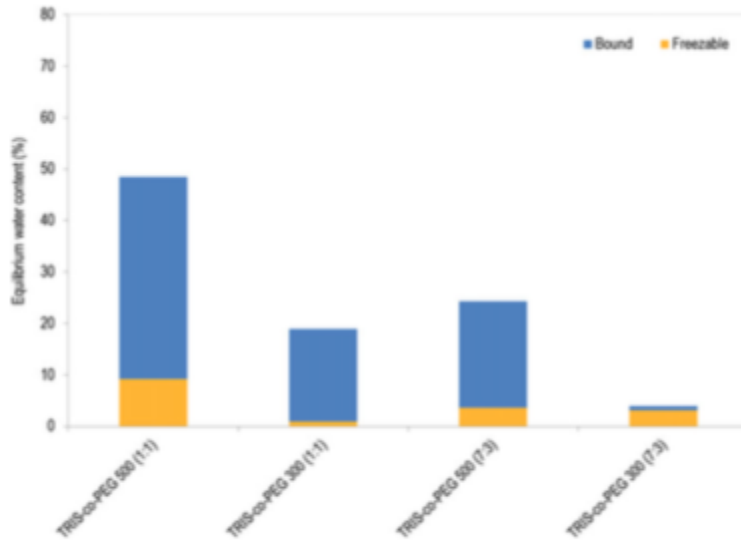


Figure 11. Correlation between the number of moles of ethylene oxide in each material and the corresponding equilibrium water content.

Given the linear relationship between PEG and EWC (Figure 12), and correlation between PEG content and the type of water, it was postulated that there may be a linear relationship between PEG and the bound water. This was confirmed in Figure 13 where a strongly linear ($R^2 \approx 0.99$) relationship is seen. Overall, this data indicates the strong influence of PEG on the amount of water and the types of water that are present in each hydrogel.

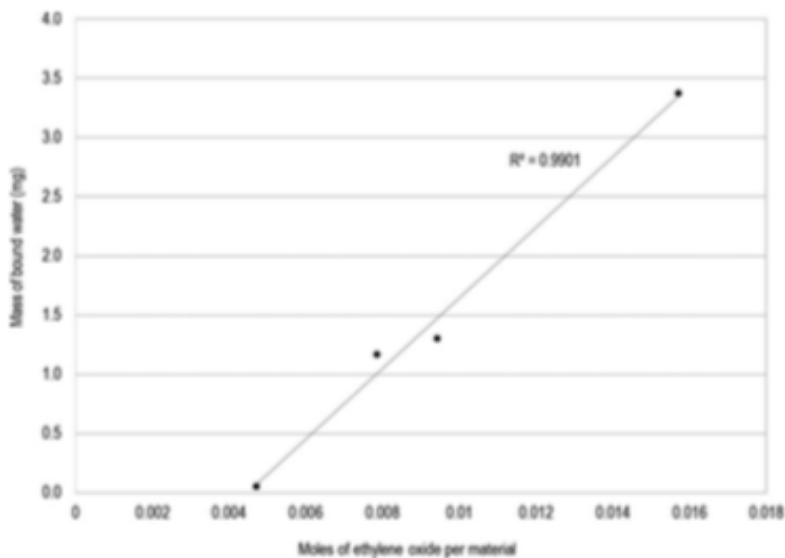


Figure 12. Relationship between the number of moles of ethylene oxide units and the amount of bound water.

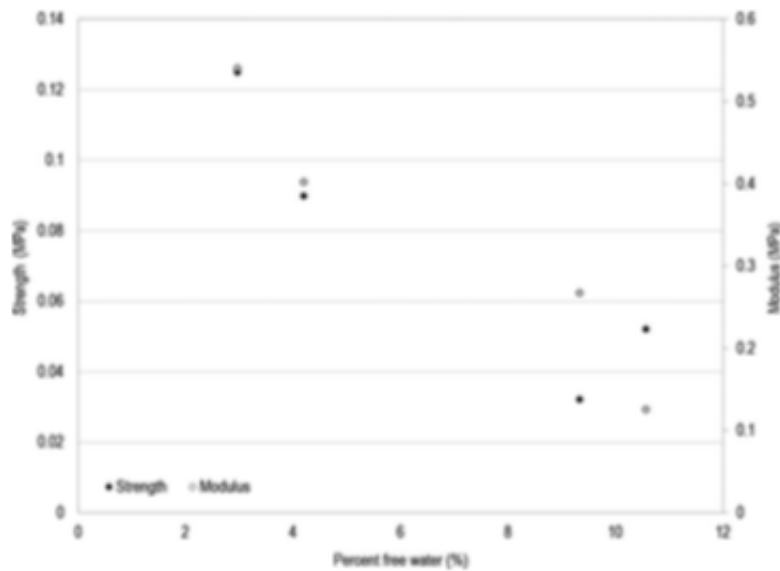


Figure 13. Relationship between the mechanical properties and amount of free water (% of EWC) in each hydrogel.

Relationship between mechanical properties and water

Mechanical testing showed interesting results that did not directly correlate to the amount of TRIS in the hydrogels (Figure 5). It was postulated that the amount of each type of water may be influencing the strength and modulus. Specifically, the amount of free water in each material could reduce mechanical properties due to its weak association only with itself, leading to areas of the hydrogel which are less strong and elastic. In Figure 13, the material strength and elasticity was plotted against the amount of free water to examine this relationship. The correlation with elastic modulus is quite linear ($R^2 \approx 0.92$), while the relationship with material strength is less linear ($R^2 \approx 0.84$). Thus the data suggests the amount of free water in each material may be an influencing factor for the tensile strength and elasticity of the material, in addition to the TRIS content.

Drug release

The release of hydrophilic drugs was examined to understand the influence of PEG properties on drug release. Specifically, the release of two structurally similar, very hydrophilic aminoglycoside antibiotics was examined from each material type. Overall, the total 24hour release amount for each drug was found to be similar for each formulation.

The release of tobramycin (Figure 14) showed the largest burst from material with the longest PEG chain (PEG₅₀₀) and the highest PEG concentration (50%); the lowest burst of drug was seen from materials containing PEG₃₀₀. Altered, more gradual drug release was seen for up to 6 hours with TRIS-co-PEG₅₀₀ (7:3). This gradual release data showed poor fit when examined against first order release kinetics (data not shown), however it showed good fit against the Higuchi diffusion model for the first 6 hours (Table 8).

The experiment was repeated with amikacin (a structurally similar aminoglycoside) to determine whether the results would be maintained with another highly hydrophilic and hydrogen-bonding-capable small molecule. As seen in Figure 15, the same release patterns were noted as with tobramycin release.

Overall the data indicates that the PEG structure (concentration and molecularweight) is an influencing factor in hydrophilic drug release from the material.

Further plotting of the data on a Higuchi plot (Table 8), demonstrated a good fit over the first 6 hours.

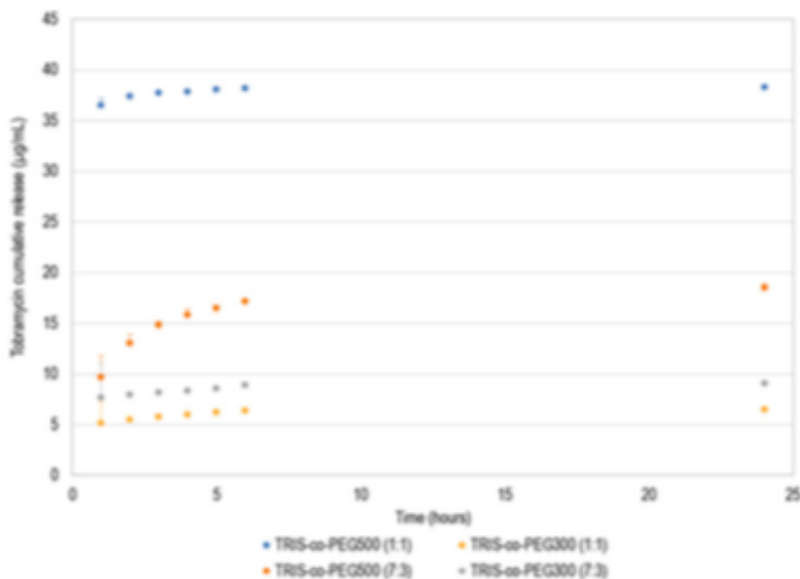


Figure 14. Release of tobramycin from silicone hydrogels, measured over 24 hours (stdev, n = 4).

Table 8. The fit (R^2) to the Higuchi model ($t^{1/2}$) of TRIS-co-PEG₅₀₀ (7:3) drug release over the first six hours.

	Tobramycin Release (R^2)	Amikacin Release (R^2)
TRIS-co-PEG ₅₀₀ (7:3)	0.97	0.99

Overall the data indicates that the PEG structure (concentration and molecular weight) is an influencing factor in hydrophilic drug release from the material.

Discussion

While contact lenses have the potential to increase the on eye residence time of drugs for treating a host of different conditions, they have not reached their potential in terms of application. Silicone hydrogels in particular have the potential to better control the release of drugs compared to conventional materials and thus TRIS was chosen as the hydrophobic component of a novel silicone hydrogel material. Then, the specific objective of this work was to investigate the unique structure-function relationship between PEG and water, when PEG is chemically incorporated as part of a silicone hydrogel material and to determine whether the incorporation of PEG could be used to control the release of hydrophilic drugs, presumably through hydrogen bonding. Together, a novel silicone hydrogel was created based on the methacrylated macromers TRIS and PEG, and the properties of the materials were assessed through chemical characterization, surface characterization and bulk characterization.

Successful synthesis of TRIS and PEG-based hydrogels

It was found that TRIS and PEG macromers can be directly co-polymerized to produce a highly wettable material with no macroscopic phase separation. While it can be difficult to directly incorporate polymers of opposing solubility, in this case, the use of low molecular weight PEG and the addition of a small amount of IPA as a solvent (which can be easily removed), resulted in materials with appropriate optical clarity, refractive index, and high transmittance. Due to the relatively short PEG chains chosen, it is likely that PEG is able to adopt non-polar conformations [54, 55], resulting in more compatibility with adjacent TRIS molecules. Of note, the oxygen permeability of these materials was not measured and it may be necessary to incorporate an additional siloxane macromer to generate materials with better potential oneye properties.

Influence of PEG structure on water content

The magnitude of the effect of PEG molecular weight on the equilibrium water content (EWC) was unexpected. At the same molarity, there was more than a 30% increase in EWC in PEG₅₀₀ formulations versus PEG₃₀₀ formulations. This was despite only an approximately 4.5 ethylene oxide (EO) unit difference between PEG₅₀₀ and PEG₃₀₀ chains. However, developing materials based on molar concentration in this conjugated macromer system results in differing numbers of EO units per material. Therefore, the variables of molecular weight and concentration cannot be independently studied. In order to fully understand the effects of PEG on the material properties then, a structurally deeper perspective must be taken – looking at the effect of the overall number of EO subunits on material properties. With the knowledge that each EO subunit of PEG can hydrogen-bond 2-3 water molecules, the relationship between EO units and the EWC/swelling was explored. Indeed, in [Figure 9](#), a highly correlative, linear relationship was seen between the number of EO units per material, and the EWC ($R^2/40.99$) and swelling ($R^2/40.96$). This data indicate that EWC and swelling are directly dependent on the number of EO subunits in the material introduced through the incorporation of PEG. Future work in modelling the equilibrium water content and the affine deformation of network chains (based on Flory-Rehner theory), will provide deeper understanding of the interactions between polymer and water, and the parallel effects on elasticity/tensile properties. Taken together, these results indicate that the water content of TRIS-co-PEG hydrogels may be finely tunable, simply by altering the number of EO units. Future work should continue to explore this relationship, starting with the manufacture of a TRIS-co-PEG material based on the calculated number of EO units required for a desired EWC. Given that EO units can be introduced by altering either the PEG concentration or the PEG molecular weight, the effect of one approach over another could then be explored, as there may be added opportunity for tuning the material through adjusting this variable as well.

The relationship with water showed some interesting results when related to the presence of PEG ([Figure 11](#)). With increasing EO content the amount of bound water increased – this was expected given that increased EO content provides increased binding sites. However surprisingly, each water profile was unique. For example, the PEG₃₀₀ (7:3) formulation showed negligible bound water, while the PEG₅₀₀ (7:3) formulation showed the least amount of freezable water.

Thus the water profiles are not simply related to either the EWC or the EO content, rather the data suggests an influence of the PEG hydrogen-bonding ability and EWC/swelling together. In the case of the PEG₃₀₀ (7:3) formulation, it has the inherent ability to bind water (as a result of the presence of PEG), but it also has a very small EWC/swelling (~5/6% respectively). This low EWC/swelling suggests that water does not penetrate deeply into the material, leading to it being mostly associated at the surface layers, rather than throughout the material (and bound to PEG). Then, the amount of bound water is negligible and the majority of water is free (or loosely bound) at the surface (and this is indeed observed in the thermogram). Using this same approach to understand the PEG₅₀₀ (7:3) data, we see the EWC/swelling is larger (~28/40% respectively), suggesting that a larger amount of bound water is present in the material and available for binding with PEG – and this larger bound mass of water is indeed observed according to the thermogram. At the same time, because of the longer chain length of PEG₅₀₀, water found at the surface layers may be more likely to be associated with the PEG, rather than freely or loosely bound to it, leading to less freezable water being detected in the system.

Hydrophilic drug release is influenced by PEG structure, and the unique types of water in each material

The controlled release of highly hydrophilic molecules from a hydrogel remains a challenge. It was hypothesized that the structured interactions between PEG and drug/water can be used to control movement through the material and influence drug release. Specifically the investigated hydrophilic drugs contain multiple amine groups and hydroxyl groups capable of hydrogen bonding, and thus it is reasonable to hypothesize that once drug is in the material, it is able to hydrogen bond with the EO groups on PEG, and have release altered. Thus, the release of the hydrophilic ophthalmic drug tobramycin (and structurally similar amikacin) from TRIS-co-PEG hydrogels was investigated.

The release trends were similar across both drugs tested. For most formulations, an early release was seen, followed by a small, residual release of remaining drug. This is a commonly observed release curve for hydrophilic compounds in hydrogels. However, with TRIS-co-PEG₅₀₀ (7:3), a more gradual release was seen over 6 hours, with some additional release over 24 hours. Somewhat unexpectedly, the drug release over the first 6 hours release fits the Higuchi drug release model for all formulations. Higuchi kinetics are based on a model

where a solid drug is incorporated during fabrication and is dispersed throughout a polymer matrix. The release first begins with drug located closest to the surface. Then, as water enters the matrix, deeper drug is able to be dissolved and released. Given that in the investigated materials the drug was loaded by soaking the silicone hydrogels in drug solution, Higuchi release kinetics would indicate that the hydrogen bonding ability of PEG can control the movement of water and drug resulting in the release observed.

If the state of water in the hydrogels is taken into account, this provides us with the ability to view the material release kinetics from a perspective that aligns with and helps to explain the Higuchi fit seen. Similar to the equilibriums that occur in a Higuchi model – as free water enters the system, free drug not hydrogen-bonded to PEG, is first released. This can be conceptually related to the initial equilibrium that occurs in the Higuchi model at the surface of the material. Then, as free water is exchanged with loosely bound water and drug, the associated drug then becomes free drug and is able to be released from the system. This is similar to the second equilibrium of a Higuchi release model, where more deeply embedded drug is dissolved and then able to be released. Finally, as free water continues to penetrate throughout the material, it is also exchanged with the tightly hydrogen bonded water and drug found at the PEG chains. This is related to the third equilibrium stage of Higuchi release where most deeply embedded drug is dissolved, and must navigate through the material and is then released.

This system provides a good understanding of the equilibriums that are suggested to occur based on the Higuchi fit that is seen. However the water profile (free, intermediate, bound) of each formulation is dependent on both the presence of PEG, but also the EWC/swelling of each material (as described earlier). By taking both into account, we can then comprehend the data more fully. For example, PEG₅₀₀ (1:1) shows the most amount of bound water (Figure 11), but the release data shows negligible release after the first 3 hours. It would be expected that this formulation would show the longest controlled release. However, the high EWC of the material (~60%) provides a large area for water exchange, leading to a more rapid exchange of free water with the bound drug at the polymer, and thus a more rapid depletion of the stored/bound drug within the material. In contrast, the PEG₅₀₀ (7:3) formulation has less bound water but more gradual release, and as the data indicates, this is likely due to the lowered EWC of the material, reducing the area available for water exchange within the

polymer and reducing the rate at which the bound water and loosely bound water are released.

This analytic approach also provides understanding of the release from the PEG₃₀₀ formulations. PEG₃₀₀ (1:1) has more loosely and tightly bound water than the PEG₃₀₀ (7:3) formulation, forming the expectation for greater overall drug release from the (1:1) formulation. However, drug release amounts are observed to be fairly similar across the two formulations. Considering that the ~19% EWC of the (1:1) formulation provides low area available for water exchange (in comparison to PEG₅₀₀ formulations), the amount of loosely and tightly bound water would be very slow to equilibrate with free water, creating the small initial burst and very gradual release over time. Taken together, the data demonstrates that the presence of PEG in the TRIS-co-PEG hydrogels provides the ability to alter the release of very hydrophilic small molecules through its ability to hydrogen-bond with water and hydrophilic small molecules – where the effects of hydrogen-bonding can be understood through the unique water profiles and EWCs of each formulation.

It is important to note that additional features likely contribute to the effects seen, and could also be explored to understand how to alter hydrophilic drug release from these materials. For example, in materials containing less EO (and therefore higher TRIS), there will be a lowered driving force of hydrophilic drug into the material, and an increased driving force out. The altered loading values contribute to the overall amounts released. It may also be possible that the gradual release is influenced by the physical barrier presented by the TRIS component in the presence of PEG-created water channels. Specifically, the hydrogels contain a significant fraction of hydrophobic TRIS which may obstruct the formation of long, direct channels of hydrated PEG throughout the material. As a result, hydrophilic drug solution that is loaded into the gel must diffuse out by navigating through channels that may be open or obstructed based on the movement of both TRIS and PEG chains. This obstructed pathway out of the material may contribute to the more sustained, controlled release of drug that is seen in formulations showing more gradual release, such as the PEG₅₀₀ (7:3) formulation. Likewise with a lower TRIS content, larger burst release can be explained because the equilibrium water content is significantly greater, so any channels are much larger (and less obstructed) and drug release is no longer controlled. Therefore the addition of a siloxane component into the gels may also further prolong the release by creating a more tortuous barrier to drug

diffusion.

Conclusion

In this work, a novel hydrogel was developed. It was demonstrated that macromers of opposing solubility can be directly co-polymerized to produce optically transparent materials with no phase separation when hydrated in PBS. In addition, the resulting materials were found to be highly hydrophilic, and yet could be reformulated to maintain desired properties, with a water content that was tunable between ~5 to 60% while maintaining a highly hydrophilic contact angle of approximately 40°. This tuning is thought to be possible based on the structure of PEG, and specifically the number of EO units introduced by PEG. Finally, the controlled release of hydrophilic antibiotics from TRIS-co-PEG hydrogels was demonstrated, with Higuchi-based kinetics providing a conceptual understanding of the molecular-level equilibria that appear to be occurring between the hydrogen-bonded drugs and free drugs. Further incorporation of EWC/swelling data provides a basis for understanding the unique drug release profiles of each formulation. Overall, the development and investigation of TRIS-co-PEG hydrogels in this work provides a novel platform for expanding the development and understanding of PEG as a biomaterial with the ability to control drug release kinetics upon incorporation into materials.

Acknowledgements

Thank you to Dr. Talena Ramberran for consultation for solution state NMR. Thank you to Dr. Mike Thompson for use of the DSC and to Heera Meerway for training. Thank you to Dr. Glynis DeSilveira, who performed the Electron Microscopy analysis described in this paper at the Canadian Centre for Electron Microscopy at McMaster University, which is supported by NSERC and other government agencies.

Disclosure statement

No potential conflict of interest was reported by the authors.

ORCID

Ivana Postic <http://orcid.org/0000-0003-4177-3838>

Heather Sheardown <http://orcid.org/0000-0002-5404-635X>

References

- [1] McKenzie M, Betts D, Suh A, et al. Hydrogel-based drug delivery systems for poorly water-soluble drugs. *Molecules*. 2015;20:20397–20408.,
- [2] Lee SC, Kwon IK, Park K. Hydrogels for delivery of bioactive agents: A historical perspective. *Adv Drug Deliv Rev*. 2013;65:17–20.
- [3] Siegel RA, Rathbone MJ. Overview of controlled release mechanisms. In: Siepmann J, Siegel RA, Rathbone MJ, editors. *Fundamentals and Applications of Controlled Drug Delivery*. *Advances in Delivery Science and Technology*. New York: Springer; 2012: 19–44.
- [4] Huang X, Brazel CS. On the importance and mechanisms of burst release in matrix-controlled drug delivery systems. *J Control Release*. 2001;73:121–136. Jun.
- [5] Peng CC, Kim J, Chauhan A. Extended delivery of hydrophilic drugs from silicone hydrogel contact lenses containing Vitamin E diffusion barriers. *Biomaterials*. 2010;31: 4032–4047.
- [6] Lee D, Cho S, Park HS, et al. Ocular drug delivery through pHEMA-Hydrogel contact lenses co-loaded with lipophilic vitamins. *Nat. Publ. Gr*. 2016;6:1–8.
- [7] Ratner BD. Reducing capsular thickness and enhancing angiogenesis around implant drug release systems. *J. Control. Release*. 2002;78:211–218.
- [8] Calo_E, Khutoryanskiy VV. Biomedical applications of hydrogels: A review of patents and commercial products. *Eur. Polym. J*. 2015;65:252–267.
- [9] Hoare TR, Kohane DS. Hydrogels in drug delivery: Progress and challenges. *Polymer (Guildf)*. 2008;49:1993–2007.
- [10] Coelho JF, Ferreira PC, Alves P, et al. Drug delivery systems: Advanced technologies potentially applicable in personalized treatments. *Epma J*. 2010;1:164–209.
- [11] Ige OO, Umoru LE, Aribo S. Natural products: A minefield of biomaterials. *ISRN Mater Sci*. 2012;2012:1–20.
- [12] Maitz MF. Applications of synthetic polymers in clinical medicine. *Biosurface Biotribol*. 2015;1:161–176.
- [13] StamatialisDF, PapenburgBJ, Giron_esM, et al. Medical applications of membranes: Drug delivery, artificial organs and tissue engineering. *J Memb Sci*. 2008;308:1–34.

- [14] Berger J, Reist M, Mayer JM, et al. Structure and interactions in covalently and ionically crosslinked chitosan hydrogels for biomedical applications. *Eur J Pharm Biopharm.* 2004;57:19–34.
- [15] Ashley GW, Henise J, Reid R, et al. Hydrogel drug delivery system with predictable and tunable drug release and degradation rates. *Proc Natl Acad Sci USA.* 2013;110:2318–2323.
- [16] Brandl F, Hammer N, Blunk T, et al. Biodegradable hydrogels for time-controlled release of tethered peptides or proteins. *Biomacromol.* 2010;11:496–504.
- [17] Korogiannaki M, Guidi G, Jones L, et al. Timolol maleate release from hyaluronic acid-containing model silicone hydrogel contact lens materials. *J Biomater Appl.* 2015;0:1–16.
- [18] Hsu K-H, Gause S, Chauhan A. Review of ophthalmic drug delivery by contact lenses. *J Drug Deliv.* 2014;24:123–135.
- [19] Puttipipatkachorn S, Nunthanid J, Yamamoto K, et al. Drug physical state and drug-polymer interaction on drug release from chitosan matrix films. *J Control Release.* 2001;75:143–153.
- [20] Hui A, Willcox M, Jones L. In vitro and in vivo evaluation of novel ciprofloxacin-releasing silicone hydrogel contact lenses. *Invest Ophthalmol Vis Sci.* 2014;55:4896.
- [21] Alvarez-Lorenzo C, Hiratani H, Gomez-Amoza JL, et al. Soft contact lenses capable of sustained delivery of timolol. *J Pharm Sci.* 2002;91:2182–2192.
- [22] Alvarez-Lorenzo C, Yan~ez F, Barreiro-Iglesias R, et al. Imprinted soft contact lenses as norfloxacin delivery systems. *J Control Release.* 2006;113:236–244.
- [23] Hiratani H, Alvarez-Lorenzo C. Timolol uptake and release by imprinted soft contact lenses made of N, N-diethylacrylamide and methacrylic acid. *J Control Release.* 2002; 83:223–230.
- [24] Schmidt DR, Waldeck H, Kao WJ. Protein adsorption to biomaterials. In: Puleo D., Bizios R. (eds) *Biological Interactions on Materials Surfaces.* New York: Springer; 2009; 2–17.
- [25] Soltys-Robitaille CE, Ammon DM, Valint PL, et al. The relationship between contact lens surface charge and in-vitro protein deposition levels. *Biomaterials.* 2001;22:3257–3260.
- [26] Anderson JM. Mechanisms of inflammation and infection with implanted devices.

Cardiovasc Pathol. 1993;2:33–41.

[27] Anderson JM, Rodriguez A, Chang DT. Foreign body reaction to biomaterials. *Semin Immunol.* 2008;20:86–100.

[28] Papageorgiou GZ, Papadimitriou S, Karavas E, et al. Improvement in chemical and physical stability of fluvastatin drug through hydrogen bonding interactions with different polymer matrices. *Curr Drug Deliv.* 2009;6:101–112.

[29] Ozeki T, Yuasa H, Kanaya Y. Application of the solid dispersion method to the controlled release of medicine. IX. Difference in the release of flurbiprofen from solid dispersions with poly(ethylene oxide) and hydroxypropylcellulose and the interaction between medicine and polymers. *Int J Pharm.* 1997;155:209–217.

[30] Huang Y, Dai W-G. Fundamental aspects of solid dispersion technology for poorly soluble drugs. *Acta Pharm Sin B.* 2014;4:18–25.

[31] Van Duong T, Reekmans G, Venkatesham A, et al. Spectroscopic investigation of the formation and disruption of hydrogen bonds in pharmaceutical semicrystalline dispersions. *Mol Pharmaceutics.* 2017;14:1726–1741.,

[32] Chou S-F, Woodrow KA. Relationships between mechanical properties and drug release from electrospun fibers of PCL and PLGA blends. *J Mech Behav Biomed Mater.* 2017; 65:724–733.

[33] Sanabria-DeLong N, Agrawal SK, Bhatia SR, et al. Controlling hydrogel properties by crystallization of hydrophobic domains. *Macromolecules.* 2006;39:1308–1310.

[34] Tranoudis I, Efron N. Water properties of soft contact lens materials. *Contact Lens Anterior Eye.* 2004;27:193–208.

[35] Nicolson PC, Vogt J. Soft contact lens polymers: an evolution. *Biomaterials.* 2001;22: 3273–3283.

[36] Liu K-J, Parsons JL. Solvent effects on the preferred conformation of Poly(ethylene glycols). *Macromolecules.* 1969;2:529–533.

[37] Maxfield J, Shepherd IW. Conformation of poly(ethylene oxide) in the solid state, melt and solution measured by Raman scattering. *Polymer (Guildf).* 1975;16:505–509.

[38] Alcantar N. A, Aydil ES, Israelachvili JN. Polyethylene glycol-coated biocompatible surfaces. *J Biomed Mater Res.* 2000;51:343–351.

[39] Lin C, Yeh Y, Lin W, et al. Novel silicone hydrogel based on PDMS and PEGMA for contact lens application. *Colloids Surf B Biointer.* 2014;123:986–994.

- [40] Emoto K, Van Alstine JM, Harris JM. Stability of Poly (ethylene glycol) graft coatings. *Langmuir*. 1998;14:2722–2729.
- [41] Tobrex P, Tobrexan P. “TOBREX^{VR} and TOBREXAN^{VR} Product Monograph 193426 17MAY2016-00 2 PRODUCT MONOGRAPH,” pp. 1–22.
- [42] Kernt K, Martinez M, Bertin D, et al. A clinical comparison of two formulations of tobramycin 0.3% eyedrops in the treatment of acute bacterial conjunctivitis. *Eur J Ophthalmol*. 2005;15(5):541–549.
- [43] Desai S. Ocular pharmacokinetics of tobramycin. *Int Ophthalmol*. 1993;17:201–210.
- [44] Katime I. Swelling properties of new hydrogels based on the dimethyl amino ethyl acrylate methyl chloride quaternary salt with acrylic acid and 2-methylene butane-1,4-dioic acid monomers in aqueous solutions. *Mater Sci Appl*. 2010;1:162–167.
- [45] Ping ZH, Nguyen QT, Chen SM, et al. States of water in different hydrophilic polymers DSC and FTIR studies. *Polymer (Guildf)*. 2001;42:8461–8467.
- [46] Tekkeli SEK, O€nal A, Sa!ırlı AO. Spectrofluorimetric determination of tobramycin in human serum and pharmaceutical preparations by derivatization with fluorescamine. *Luminescence*. 2014;29:87–91.
- [47] Udenfriend S, Stein S, Bo€hlen P, et al. Fluorescamine: A reagent for assay of amino acids, peptides, proteins, and primary amines in the picomole range. *Science*. 1972;178: 871–872.
- [48] Thermo Fisher Scientific. NanoDrop 3000 Protocol Manual Fluorescamine Protein Assay. Wilmington, Delaware, US. Available at <http://tools.thermofisher.com/content/sfs/manuals/Fluorescamine-protocol.pdf>
- [49] Hosaka S, Yamada A, Tanzawa H, et al. Mechanical properties of the soft contact lens of poly(methyl methacrylate-N-vinylpyrrolidone). *J Biomed Mater Res*. 1980;14: 557–566.
- [50] Kim J, Conway A, Chauhan A. Extended delivery of ophthalmic drugs by silicone hydrogel contact lenses. *Biomater*. 2008;29:2259–2269.
- [51] Bhamra TS, Tighe BJ. Mechanical properties of contact lenses: The contribution of measurement techniques and clinical feedback to 50 years of materials development. *Contact Lens Anterior Eye*. 2017;40:70–81.
- [52] Tighe BJ. A decade of silicone hydrogel development. *Eye Contact Lens Sci. Clin*.

Pract. 2013;39:1.

[53] Gonz_alez-M_eijomeJM,LiraM,Lo_pez-AlemanA,etal.Refractiveindexandequilibrium water content of conventional and silicone hydrogel contact lenses. *Oph Phys Optics*. 2006;26:57–64.

[54] Milton Harris J, Zalipsky S. Poly(ethylene glycol) chemistry and biological applications, vol. 680. Washington (DC): American Chemical Society; 1997.

[55] Israelachvili J. The different faces of poly(ethylene glycol). *Proc Natl Acad Sci USA*. 1997;94:8378–8379.